ACS APPLIED MATERIALS & INTERFACES

Research Article

www.acsami.org

Antifogging and Antireflection Coatings Fabricated by Integrating Solid and Mesoporous Silica Nanoparticles without Any Post-Treatments

Ligang Xu[†,‡] and Junhui He*[,†]

[†]Functional Nanomaterials Laboratory, Key Laboratory of Photochemical Conversion, Optoelectronic Materials, Technical Institute of Physics, Chemistry, Chinese Academy of Sciences, Zhongguancundonglu29, Haidianqu, Beijing 100190, China

[‡]Graduate University of the Chinese Academy of Sciences, Beijing 100049 China

Supporting Information

ABSTRACT: Antifogging and -reflection coatings were fabricated on glass and poly(methyl methacrylate) (PMMA) substrates by integrating solid silica nanoparticles of 25 nm (S-25) and mesoporous silica nanoparticles (MSNs) of 45 nm via layer-by-layer assembly without any post-treatments. Superhydrophilicity and a maximum transmittance of 98.5% in the visible spectral range was achieved for the $(PDDA/S\text{-}25)_4/(PDDA/MSNs)$ coating deposited on slide glass. The maximum transmittance even reached as high as 99.3% in the visible spectral range by applying a coating of $(PDDA/S\text{-}25)_8/(PDDA/MSNs)$ on PMMA substrate. Scanning and transmission electron microscopy were used to observe the morphology and structure of nanoparticles and coating surfaces. Optical properties were characterized by UV−visible spectrophotometer. Surface wettability was studied by a contact angle/interface system. The influence of mesopores was also discussed on the transmission and wetting properties of coatings. The high porosity of mesoporous nanoparticles and loose stacking of solid and mesoporous nanoparticles are considered to significantly contribute to the enhancements of both light transmission and hydrophilicity.

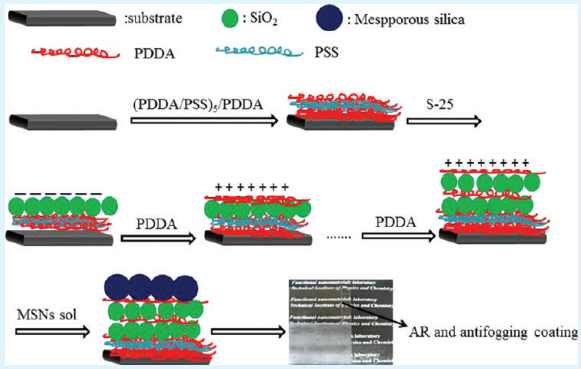

KEYWORDS: *antireflection, superhydrophilic, antifogging, mesoporous silica nanoparticle, solid silica nanoparticle, coating*

INTRODUCTION

Antireflective (AR) coatings have important applications on glasses, lenses, and solar cells.[1−5] The principle of antireflection is the interference of the reflected light from the air-coating and coating-substrate interfaces. Thus, the AR coatings should exhibit a reflective index between those of air and substrate. Generally, an ideal homogeneous single-layer AR coating should satisfy the following conditions: the thickness of coating should be $\lambda/4n_c$, where λ is the wavelength of incident light, and n_c is the refractive index of coating; $n_c = (n_a n_s)^{1/2}$, where n_a and n_s are the refractive indices of air and substrate, respectively.[6] Nanoporous films with a low refractive index of ∼1.22 and a thickness of one-quarter of an appropriate visible wavelength are frequently used as AR coatings on glass or transparent plastic substrates with a refractive index of ∼1.5.[1−5,7]

Meanwhile, antifogging coatings, which can prevent water condensation on substrates, are of great importance in a variety of practical applications, including mirrors, glasses, goggles, face masks, windows for vehicles, and solar cells. Superhydrophilic coatings, on which water contact angle can reach less than 5° within 0.5 s, can effectively suppress the fogging behavior by rapid spread of condensing water droplets on their surface and thus eliminating light scattering by water droplets.[8]

Coatings that integrate antireflective and antifogging properties are highly desired in automobile windshields, eyeglasses, swimming goggles, periscopes, lenses in laparoscopes, windows of high rise buildings, and solar cells.

Layer-by-Layer (LbL) assembly[9] has proven to be a simple and effective way to fabricate various kinds of coatings.[10,11] It could provide sufficient control over the thickness and structure of coating to achieve highly antireflective and superhydrophilic properties.[12−15] We previously reported that solid silica nanoparticles were used to fabricate highly antireflective and superhydrophilic coatings via LbL assembly followed by post-treatment. For example, highly antireflective and superhydrophilic coatings were fabricated from solid silica nanoparticles of two different sizes (150 and 30 nm) by LbL assemble followed by calcination.[16] Very recently, we fabricated silica nanoparticles coatings on PMMA substrates via LbL assembly followed by oxygen plasma treatment, which showed

Received: April 14, 2012
Accepted: June 4, 2012
Published: June 4, 2012

antireflection (T_{max} = 98.5%) and superhydrophilicity.[17] The fabrication of antireflective coatings from solid silica nanoparticles usually need post-treatments such as calcination or oxygen plasma treatment to achieve superhydrophilicity. Calcination at high temperature is, however, not suitable for substrates of low glass-transition temperature, including poly (methyl methacrylate) (PMMA). On the other hand, oxygen plasma treatment would decrease the transmittance of coatings.[17]

Mesoporous and hollow silica nanoparticles with low refractive index were also used to fabricate antireflective coatings on substrates.[15,18−20,31,32] Coatings fabricated by mesoporous silica nanoparticles, to a certain extent, improved both antireflective and wetting properties because of their low refractive index and high porosity. When such mesoporous silica nanoparticles coatings were exposed to ambient air conditions, however, the moisture in air would be absorbed into the mesopores, which would modify their refractive index and thus optical properties. Coatings fabricated on PMMA substrates using hollow silica nanoparticles without any post-treatments were highly antireflective, the maximum transmittance increasing from 92 to 98%.[20] However, it is not known whether or not these coatings without any post treatments showed superhydrophilic and antifogging properties.

Herein we report the LbL fabrication of highly antireflective and antifogging coatings by integrating solid and mesoporous silica nanoparticles (MSNs) on glass or PMMA substrates. Deposition of one or two layers of PDDA/MSNs on $(PDDA/S\text{-}25)_m$ multilayers coated glass or PMMA substrates gave $(PDDA/S\text{-}25)_m/(PDDA/MSNs)_n$ coatings, which improved both antireflective and wetting properties without applying any post treatment as compared with coatings fabricated only by solid silica nanoparticles. The maximum transmittance of coated slide glasses is as high as 98.5%, whereas uncoated slide glass is only 91.3%. Meanwhile, the maximum transmittance reached as high as 99.3% on PMMA substrates (92.0%). All the coatings on PMMA or slide glass substrates have excellent superhydrophilicity. To the best of our knowledge, previous works used either solid silica nanoparticles or mesoporous silica nanoparticles for fabrication of antifogging and antireflective coatings. The current work first fabricated antireflective and antifogging coatings by integrating both solid and mesoporous silica nanoparticles without any post-treatments.

EXPERIMENTAL SECTION

Materials. Tetraethyl orthosilicate (TEOS, 98+%) and sodium poly(4-styrenesulfonate) (PSS, M_w = 70 000) were obtained from Alfa Aesar. 3-mercaptopropyltrimethoxysilane (MPTS, 95%) and poly(diallyldimethylammonium) chloride (PDDA, M_w = 200 000−350 000, 20 wt %) were purchased from Aldrich. Ammonia (25%), concentrated hydrochloric acid (37%), hydrogen peroxide (30%), cetyltrimethylammonium chloride (CTAC, 25 wt % in water), diethanolamine (DEA 98%), and absolute ethanol (99.5%) were purchased from Beihua Fine Chemicals. Monodisperse SiO_2 nanoparticles of ca. 25 nm in size were prepared according to the Stöber method.[21] Ultrapure water with a resistivity higher than 18.2 MΩ·cm was used in all experiments, and was obtained from a three-stage Millipore Mill-Q Plus 185 purification system (Academic)

Preparation of Mesoporous Silica Nanoparticles (45 nm). Sixty-four milliliters of water, 11.25 mL of ethanol, 10.4 mL of a 25 wt % CTAC aqueous solution, and 0.2 g of DEA were mixed and stirred in a water bath at 60 °C for 30 min. Then, 7.0 mL of TEOS (and 0.6 mL of MPTS) was added into the mixture within 2 min under stirring. The solution turned white gradually. It was stirred for additional 3 h. The surface of mesoporous silica nanoparticles (MSNs) was modified with sulfonate groups,[22] and MSNs had a ζ-potential of −36.5 mV. The MSNs modified with sulfonate groups are schematically shown in Scheme 1.

Scheme 1. Schematics of Mesoporous Silica Nanoparticle (MSN) Modified with Sulfonate

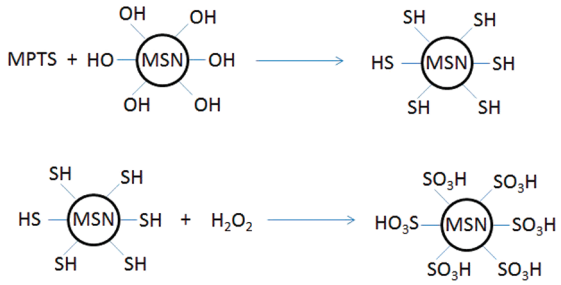

Thin Film Assembly. The procedure for preparation of antifogging antireflective coatings is described as follows. First, glass or PMMA substrates were sonicated in deionized water for at least 15 min, and then treated by oxygen plasma (84 w, 5 min) under an oxygen flow of 800 mL min^{-1}. After the oxygen plasma treatment, the glass or PMMA substrate contained surface hydroxyl groups and easily absorbed positively charged PDDA.[17] Then the cleaned substrates were alternately dipped in a PDDA (2 mg mL^{-1}) and a PSS (2 mg mL^{-1}) solution for 5 min, and redundant polyelectrolytes were removed by shaking in pure water for 2 min and rinsing for 1 min. Multilayers of $(PDDA/PSS)_5/PDDA$ were prepared and were used as a primer in all experiments. Second, the $(PDDA/PSS)_5/PDDA$ covered substrates were alternately dipped in a solid SiO_2 suspension (0.2 wt %) or MSNs suspension (0.17 wt %) and a PDDA solution (2 mg mL^{-1}) by the same procedure for an appropriate number of cycles.

Characterization. Transmission spectra in the wavelength range of 200−800 nm were recorded using a TU-1901 spectrophotometer (Beijing Purkinje General Instrument Co.). The as-prepared coatings were examined by scanning electron microscopy (SEM) on a Hitachi S-4300 scanning electron microscope operated at 10 kV. The specimens were coated with a layer of gold by ion sputtering before SEM observations. For transmission electron microscopy (TEM) observations, power products were dispersed in ethanol by sonication for 10 min, and added onto carbon-coated copper grids. After drying at 60 °C overnight, they were observed on a JEOL JEM-2100F transmission electron microscope at an acceleration voltage of 150 kV. Water contact angles (WCAs) of coating surfaces were measured at ambient temperature on a JC2000C contact angle/interface system (Shanghai Zhongchen Digital Technique Apparatus Co.). The angle precision of which is ±0.5°. Water droplets of 1 μL were dropped carefully onto the coating surfaces. Fourier Transform Infrared Spectroscopy (FTIR) spectra were recorded on a Varian Excalibur 3100 spectrometer. Nitrogen adsorption−desorption measurements were carried out using a Quantachrome NOVA 4200e surface area analyzer. The Brunauer−Emmett−Teller (BET) specific surface areas were calculated by using adsorption data in P/P_0 = 0.04−0.25 (six points collected). Pore-size distributions were estimated from adsorption branches of the isotherms by using the Barrett−Joyner−Halenda (BJH) method. Pore volumes were determined from the amounts of N_2 absorbed at a single point of P/P_0 = 0.98. For examination of antifogging property, a slide glass with porous coating was cooled at around −18 °C for 3 h in a refrigerator, and then exposed to humid laboratory air (room temperature: 20−30 °C; relative humidity: 20−40%)

RESULTS AND DISCUSSION

Morphology and Structure of Mesoporous Silica Nanoparticles. There are a number of synthetic methods[23−25] that had been used to synthesize mesoporous silica

nanoparticles. Zhang et al reported a facile synthetic route to produce monodisperse and small size (<50 nm) mesoporous silica nanoparticles in high yields.[25] Then the surface of the mesoporous silica (MSNs) was modified with sulfonate groups by the Moller method.[22] Figure 1 shows the morphology and

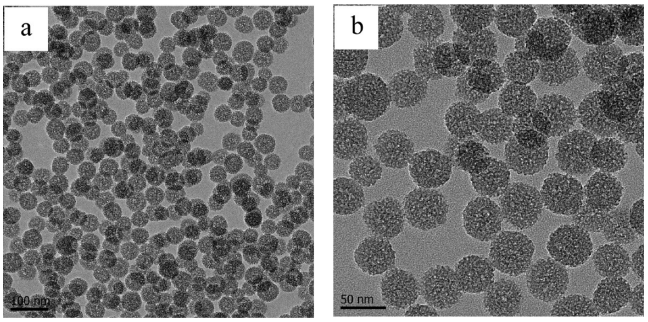

Figure 1. (a) TEM and (b) magnified TEM images of MSNs.

structure of prepared mesoporous silica nanoparticles (MSNs) modified with sulfonate groups. It can be seen that the particles are monodisperse spheres of average diameter of 45 nm in size. Figure S1 in the Supporting Information shows the FTIR spectrum of mesoporous silica nanoparticles after modification by sulfonate groups. A very strong absorption band appears at 1130 cm^{-1}, and is assigned to the stretching mode of the Si−O−Si group. In addition, two strong absorption bands appear at 980 and 800 cm^{-1}, and are associated with S═O and S−O groups, respectively. Therefore, the mesoporous silica nanoparticles were modified by sulfonate groups successfully. The sample exhibits high specific surface area, large pore volume, and narrow pore size distribution. The BET surface area, pore volume and BJH pore diameter of MSNs were estimated to be 751.3 $m^2\ g^{-1}$, 1.3 $cm^3\ g^{-1}$, and 3.8 nm, respectively.

Assembly of Multilayer Coatings on Glass Substrates. Polycation (e.g., PDDA) and polyanion (e.g., PSS) can be readily assembled on oxygen plasma treated glass substrates. As a result, a thin film of desired surface charges can be obtained on the surface of slide glasses. There are many sulfonate groups on the surface of MSNs (Scheme 1) and the point of zero charge is 2.1 for SiO_2, whereas the pH value of MSNs suspension is around 9,[26] which renders the surface of MSNs negatively charged in aqueous solution. Therefore, MSNs can be deposited alternately with PDDA on the surface of slide glass with a primer. The attractive long-range van der Waals forces, repulsive electrostatic interaction between like-charge MSNs, plus the attractive electrostatic interaction between MSNs and PDDA layer are the critical terms that govern the adsorption processes. To attain the desired roughness and voids, we deposited a varied number (one, two, three, and four) of PDDA/MSNs cycles.

Figure 2 shows the transmission spectra of control slide glass with its maximum transmittance of 91.3% in the spectral range between 300 and 800 nm and slide glasses coated with one, two, three and four cycles of PDDA/MSNs, respectively. Clearly, the slide glasses deposited with MSNs coatings show significantly enhanced transmittance compared with control slide glass. The maximum transmittances were estimated to be 93.7% at the wavelength of ca. 492 nm, 95.0% at the wavelength of ca. 512 nm, 95.5% at the wavelength of ca. 548 nm, and 94.4% at the wavelength of ca. 604 nm, respectively, for the slide glasses coated with one, two, three, and four cycles of

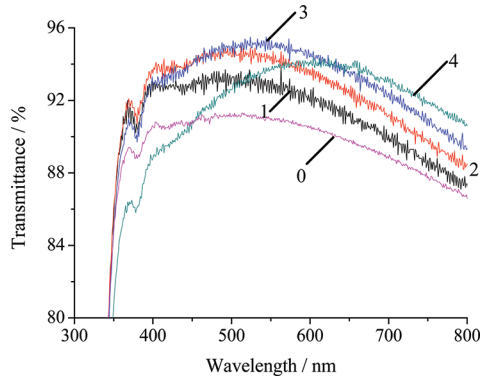

Figure 2. Transmission spectra of control slide glass (0) and slide glasses coated with one (1), two (2), three (3), and four cycles (4) of PDDA/MSNs.

PDDA/MSNs, thus exhibiting a redshift trend of the maximum transmittance wavelength.

For the initial deposition cycles, the void fraction is supposed to increase with increasing the number of deposition cycles. Void space with low refractive index (n = 1) is available for antireflective (AR) coatings.[16] However, the variation in the size and spacing of these voids would result in diffuse scattering that would degrade the quality of the AR coatings. Therefore, there would be optimal conditions to balance the void space and the concomitant diffuse scattering. For the $(PDDA/MSNs)_n$ coating, The maximum transmittance is only 95.5%. To increase the transmittance of the coatings, we fabricated coatings on substrates by integrating solid and mesoporous silica nanoparticles via LbL assembly. Deposition of one or two layers of PDDA/MSNs on $(PDDA/S\text{-}25)_m$ multilayers coated glass or PMMA substrates gave $(PDDA/S\text{-}25)_m/(PDDA/MSNs)_n$ coatings, which improved both antireflective and wetting properties without applying any post treatment as compared with coatings fabricated only by solid silica nanoparticles. For the convenience of discussion, the coating is abbreviated as "m + n" in the current paper. As shown in Figure 3, line "4 + 1" represents the transmission spectrum of $(PDDA/S\text{-}25)_4/(PDDA/MSNs)$ coated slide glass. The maximum transmittance was estimated to be 98.5% at the wavelength of ca. 477 nm. The transmittance of "4 + 2" (line "4 + 2") is lower than that of "4 + 1" probably because of enhanced diffuse scattering accompanying the increase of surface roughness (refer to Figure 5b,c).

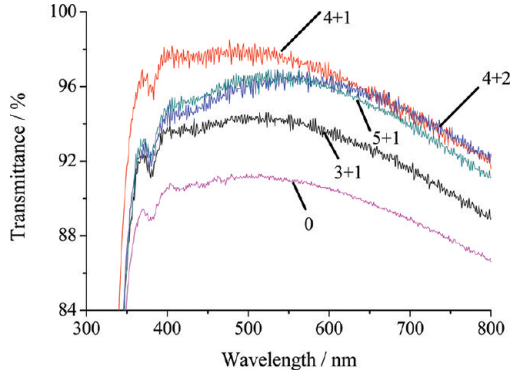

Figure 3. Transmission spectra of control slide glass (0) and slide glasses coated with $(PDDA/S\text{-}25)_m/(PDDA/MSNs)_n$ (abbreviated as "m + n").

SEM images in Figure 4 show the surface morphology of coatings deposited with one, two, three and four cycles of

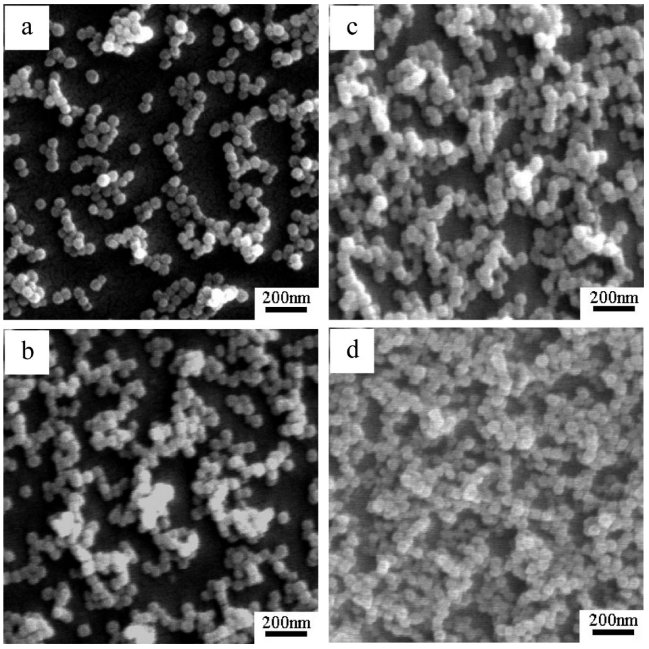

Figure 4. SEM images of MSNs coatings as prepared by deposition of (a) one, (b) two, (c) three, and (d) four cycles of PDDA/MSNs.

PDDA/MSNs. Figure 4a reveals that MSNs do not fully cover the slide glass, some MSNs stack together. By comparing the SEM images (Figure 4a–d), it can be seen that the particle packing density increases gradually and significantly as the number of deposition cycles increases. The increase in the particle packing density would lead to the increase of the refractive index of the coating. Subsequently absorbed MSNs would prefer to fill in or sit on the void spaces between MSNs, thus leading to rougher surfaces and thicker coatings.

SEM images are shown in Figure 5 for the slide glass coated with $(PDDA/S\text{-}25)_m/(PDDA/MSNs)_n$ multilayers. It can be seen that nanoparticles formed close-packed multilayers. As compared with Figure 4, nanoparticles are seen to be more crowed, and thus the void space should have decreased. Figure 5b and c show SEM images of $(PDDA/S\text{-}25)_4/(PDDA/MSNs)$ and $(PDDA/S\text{-}25)_4/(PDDA/MSNs)_2$ coatings, respectively. Clearly, surface roughness increases with increasing the number of deposition cycles of PDDA/MSNs, which may be the reason why the transmittance of "4 + 2" is lower than that of "4 + 1" (Figure 3).

According to the early theoretical works by Wenzel[27] and Quéré et al,[28,29] void fraction and surface roughness would significantly affect the wettability of a surface with water. Our previous studies[15−17,30−32] and the work by Rubner and co-workers[12,13] proved that high level of wettability of silica nanoparticles coupled with the rough and nanoporous nature of multilayer surfaces establishes ideal conditions for extreme wetting behaviors. Slide glasses coated with $(PDDA/S\text{-}25)_m/(PDDA/MSNs)_n$ multilayers showed excellent superhydrophilic property. Time-dependent changes in WCA on the surface of "$m + n$" coatings are shown in Figure 6a. The volume of water droplets for the measurements was set at 1 μL. Clearly, the WCAs on the coatings decreased with increase in time from 0 to 1000 ms, thus indicating fast spreading of water droplets.

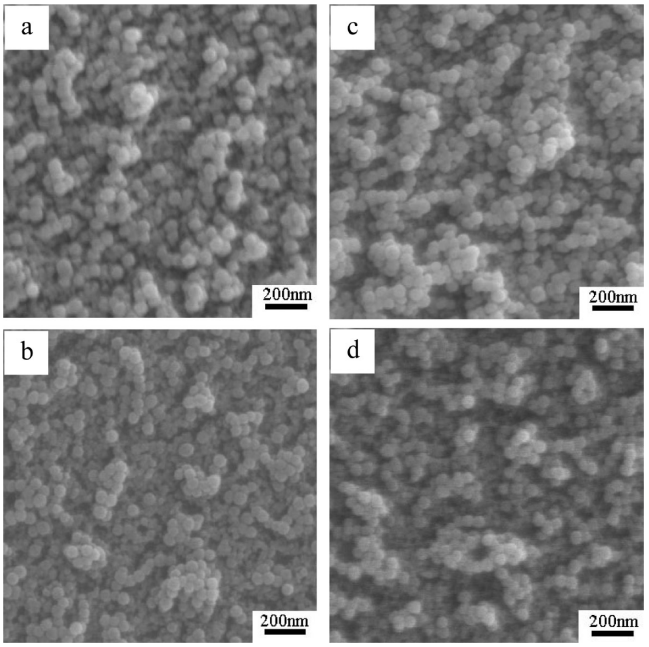

Figure 5. SEM images of $(PDDA/S\text{-}25)_m/(PDDA/MSNs)_n$ (abbreviated as "$m + n$") coatings on slide glass: (a) 3 + 1, (b) 4 + 1, (c) 4 + 2, and (d) 5 + 1.

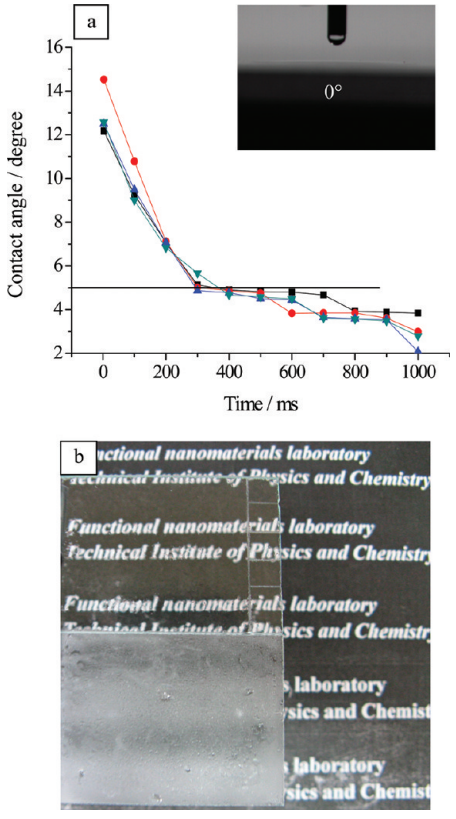

Figure 6. (a) Time-dependent changes in instant contact angle as a function of the number of $(PDDA/S\text{-}25)_m/(PDDA/MSNs)_n$ (abbreviated as "$m + n$"): 3 + 1 (■), 4 + 1(◆), 4 + 2 (▲), and 5 + 1 (▼). Water droplets of 1 μL were applied in all measurements. The inset is a water contact angle image of 4 + 1. (b) Digital image exhibiting antifogging property of slide glass coated with $(PDDA/S\text{-}25)_4/(PDDA/MSNs)$ (upper) and blank slide glass (bottom).

The inset in Figure 6a is a water contact angle image of "4 + 1" coating, which shows the shape of a sheetlike water of ca. 0°. Thus, all these coatings demonstrated superhydrophilicity (WCA less than 5° within 0.5 s or less). This may be due to the increases in the number of voids and pores and in surface roughness,[12,16] and all the increases would lead to a larger contact area between water droplet and coating, thus improving the hydrophilicity of coatings according to the Wenzel model.[27] These results agree with the SEM observations shown in Figure 5.

Superhydrophilic coatings, which can effectively prevent water condensation on transparent substrates, are of great importance in a variety of practical applications. All the superhydrophilic $(PDDA/S\text{-}25)_m/(PDDA/MSNs)_n$ coatings were found to exhibit excellent antifogging behavior. For example, a slide glass coated with $(PDDA/S\text{-}25)_4/(PDDA/MSNs)$ was cooled at −15 °C for 3 h in a refrigerator, and then exposed to humid laboratory air (relative humidity (RH): 20−40%). As shown in Figure 6b, the bare glass slide fogged immediately and the words below were blurred by strong light scattering. In contrast, the slide glass coated with $(PDDA/S\text{-}25)_4/(PDDA/MSNs)$ coatings could significantly prevent fogging by almost instantaneously spreading condensed water droplets to form a thin sheetlike water membrane. Therefore, the slide glass with $(PDDA/S\text{-}25)_4/(PDDA/MSNs)$ coating remained highly transparent and the words below were clearly seen.

AFM images in Figure S2 in the Supporting Information show the 2D and 3D images of 5 layer solid silica nanoparticles coating ($(PDDA/S\text{-}25)_5$), "4 + 1" coating and "4 + 2" coating. The rms roughness of the surfaces covered by the $(PDDA/S\text{-}25)_5$ coating, "4 + 1" coating and "4 + 2" coating were estimated to be ca. 13 nm, ca. 33 and 39 nm, respectively, from an area of 10 μm × 10 μm. Table S1 in the Supporting Information summarizes the maximum transmittance, water contact angle, and surface roughness of $(PDDA/S\text{-}25)_5$ coating, "4 + 1" coating and "4 + 2" coating. The maximum transmittance of $(PDDA/S\text{-}25)_5$ coating is 98.2% at the wavelength of ca. 458 nm, while those of the "4 + 1" and "4 + 2" coatings are 98.5% at the wavelength of ca. 477 nm and 96.9% at the wavelength of ca. 543 nm. The "4 + 1" and "4 + 2" coatings (CA 0°) shows, however, much higher wetting property compared with the $(PDDA/S\text{-}25)_5$ coating (15°). Surface roughness may influence light transmission by light scattering, and may also influence the wetting property as revealed by the Wenzel theory.[27] However, the current results indicate that surface roughness has more significant effect on the wetting property than light transmission (see Table S1 in the Supporting Information). Mesoporous silica nanoparticles with high porosity apparently improved the wetting property of coating.

Assembly of Multilayer Coatings on PMMA Substrates. $(PDDA/S\text{-}25)_m/(PDDA/MSNs)_n$ was also deposited on PMMA substrates to obtain antireflective antifogging coatings. As shown in Figure 7, bare PMMA substrate with a refractive index of 1.49 has a maximum transmittance of 92.0% in the spectral range of 300 to 800 nm. For the PMMA substrates coated with "4 + 1", "6 + 1", "8 + 1", and "9 + 1" coatings, the maximum transmittances were estimated to be 95.9% at the wavelength of ca. 515 nm, 98.9% at the wavelength of ca. 563 nm, 99.3% at the wavelength of ca. 653 nm and 99.1% at the wavelength of ca. 678 nm, respectively. The changing trends of transmission curves in Figure 7 are obviously different by changing the number of bilayers deposited, which may be related to the thickness of coating. It is known that the wavelength of the maximum transmittance of coating is related to the thickness of coating, which could be well described by the equation: $\lambda = 4n_c d$, where d is the thickness of coating, and λ is the wavelength of the maximum transmittance.[15]

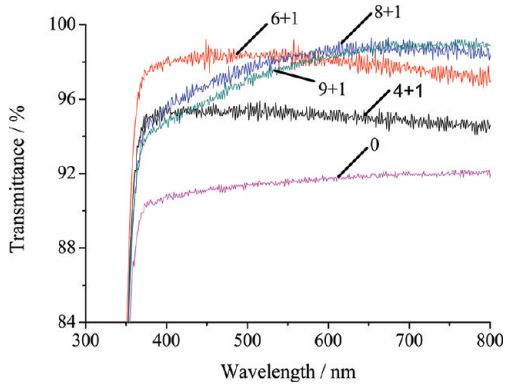

Figure 7. Transmission spectra of control PMMA substrate (0) and PMMA substrates coated with $(PDDA/S\text{-}25)_m/(PDDA/MSNs)_n$ (abbreviated as "$m + n$").

Time-dependent changes in WCA are shown in Figure 8a, and all these coatings demonstrated superhydrophilicity. As an typical example, the antifogging behavior of the $(PDDA/S\text{-}25)_8/(PDDA/MSNs)$ coating on PMMA substrate is clearly demonstrated in Figure 8b.

From our previous research,[17] the maximum transmittance of $(PDDA/S\text{-}25)_8$ coating is only 97.6% on PMMA substrate, whereas $(PDDA/S\text{-}25)_8/(PDDA/MSNs)$ is 99.3%. The static WCA on the pristine PMMA substrate is ca. 78.9°, and it is ca.44.2° on the PMMA substrate treated by oxygen plasma, The average WCA on the $(PDDA/PSS)_5/PDDA$ covered PMMA was 40.2°. The contact angle on the $(PDDA/S\text{-}25)_8$ coating was estimated to be ca. 29.0° (Figure 9a). In contrast, the contact angle was estimated to be 2.6° on the $(PDDA/S\text{-}25)_8/(PDDA/MSNs)$ coating (Figure 9b). These results indicate that the $(PDDA/S\text{-}25)_8/(PDDA/MSNs)$ coating shows a higher transmittance an more hydrophilic than that of the $(PDDA/S\text{-}25)_8$ coating on PMMA substrate.

CONCLUSIONS

In summary, by integrating solid and mesoporous silica nanoparticles, antifogging and -reflection coatings were successfully fabricated via LbL assembly without any post-treatments. The obtained $(PDDA/S\text{-}25)_m/(PDDA/MSNs)_n$ coatings on glass substrates exhibited excellent antifogging and antireflective properties. A maximum transmittance of 98.5% in the visible spectral range was achieved for the $(PDDA/S\text{-}25)_4/(PDDA/MSNs)$ coating deposited on slide glass. Antireflective and antifogging coatings could also be conveniently deposited on PMMA substrates. The maximum transmittance reached as high as 99.3% by applying a coating of $(PDDA/S\text{-}25)_8/(PDDA/MSNs)$ on PMMA substrate. The mesoporous silica nanoparticles may, however, affect light transmission under variable humidity atmosphere, which may be a drawback of these films. The current approach may provide a new route to fabrication of antireflective, superhydrophilic and antifogging coatings on substrates (e.g., polymer substrates) of low glass-transition temperature.

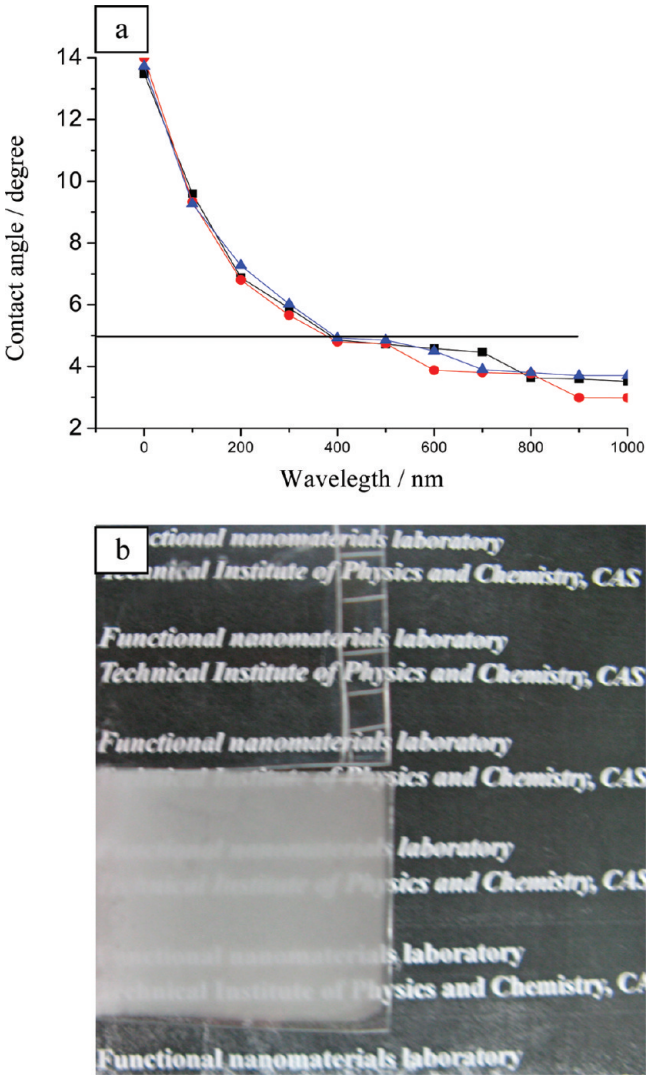

Figure 8. (a) Time-dependent changes in instant contact angle as a function of the number of $(PDDA/S\text{-}25)_m/(PDDA/MSNs)_n$ (abbreviated as "m + n"): 4 + 1 (■), 6 + 1(◆), and 8 + 1 (▲) Water droplets of 1 μL were applied in all measurements. The inset is a water contact angle image of 4 + 1. (b) Digital image exhibiting antifogging property of PMMA coated with $(PDDA/S\text{-}25)_8/(PDDA/MSNs)$ (upper) and blank PMMA substrate (bottom).

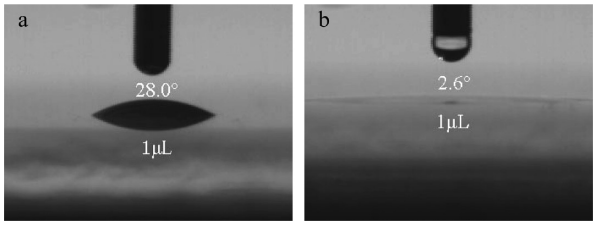

Figure 9. Images of immediate water contact angle on (a) $(PDDA/S\text{-}25)_8$ coating and (b) $(PDDA/S\text{-}25)_8/(PDDA/MSNs)$ coating, water droplets of 1 μL were applied in all measurements.

■ ASSOCIATED CONTENT

Supporting Information

FTIR spectrum of mesoporous silica nanoparticles after modification by sulfonate groups (Figure S1), Two-dimensional AFM images of (a) $(PDDA/S\text{-}25)_5$ coating, (b) "4 + 1" coating and (c) "4 + 2" coating. (d–f) Corresponding three-dimensional AFM images (Figure S2) and Maximum transmittances, wetting properties and roughness of $(PDDA/S\text{-}25)_5$ coating, "4 + 1" coating and "4 + 2" coating, respectively (Table S1). This material is available free of charge via the Internet at http://pubs.acs.org.

■ AUTHOR INFORMATION

Corresponding Author

*Fax: +86 10 82543535. E-mail: jhhe@mail.ipc.ac.cn.

Notes

The authors declare no competing financial interest.

■ ACKNOWLEDGMENTS

This work was supported by the National High Technology Research and Development Program ("863" Program) of China (Grant 2011AA050525), the Knowledge Innovation Program of the Chinese Academy of Sciences (CAS) (Grant KGCX2-YW-370, KGCX2-EW-304-2) and "Hundred Talents Program" of CAS.

■ REFERENCES

(1) Walheim, S.; Schäffer, E.; Mlynek, J.; Steiner, U. *Science* **1999**, *283*, 520–522.
(2) Hiller, J. A.; Mendelsohn, J. D.; Rubner, M. F. *Nat. Mater.* **2002**, *1*, 59–63.
(3) Hattori, H. *Adv. Mater.* **2001**, *13*, 51–54.
(4) Wu, Z.; Walish, J.; Nolte, A.; Zhai, L.; Cohen, R. E.; Rubner, M. F. *Adv. Mater.* **2006**, *18*, 2699–2702.
(5) Deng, X.; Mammen, L.; Zhao, Y.; Lellig, P.; Müllen, K.; Li, C.; Butt, H.-J.; Vollmer, D. *Adv. Mater.* **2011**, *23*, 2962–2965.
(6) Yoldas, B. E. *Appl. Opt.* **1980**, *19*, 1425–1429.
(7) Li, Y.; Zhang, J.; Zhu, S.; Dong, H.; Jia, F.; Wang, Z.; Sun, Z.; Zhang, L.; Li, Y.; Li, B.; Xu, W.; Yang, B. *Adv. Mater.* **2009**, *21*, 4731–4734.
(8) Gao, X.; Yan, X.; Yao, X.; Xu, L.; Zhang, K.; Zhang, J.; Yang, B.; Jiang, L. *Adv. Mater.* **2007**, *19*, 2213–2217.
(9) Decher, G. *Science* **1997**, *277*, 1232–1237.
(10) Zhang, X.; Chen, H.; Zhang, H. *Chem.Commun.* **2007**, 1395–1405.
(11) Quinn, J. F.; Johnston, A. P. R.; Such, G. K.; Zelikin, A. N.; Caruso, F. *Chem. Soc. Rev.* **2007**, *36*, 707–718.
(12) Lee, D.; Rubner, M.; Cohen, R. *Nano Lett.* **2006**, *6*, 2305–2312.
(13) Cebeci, F. Ç.; Wu, Z.; Zhai, L.; Cohen, R. E.; Rubner, M. F. *Langmuir* **2006**, *22*, 2856–2862.
(14) Zhang, L.; Li, Y.; Sun, J. *Langmuir* **2008**, *24*, 10851–10857.
(15) Du, X.; He, J. *Chem.—Eur. J.* **2011**, *17*, 8165–8174.
(16) Liu, X.; He, J. *J. Phys. Chem. C* **2008**, *113*, 148–152.
(17) Geng, Z.; He, J.; Xu, L. *Mater. Res. Bull.* **2012**, *47*, 1562–1567.
(18) Hoshikawa, Y.; Yabe, H.; Nomura, A.; Yamaki, T.; Shimojima, A.; Okubo, T. *Chem. Mater.* **2009**, *22*, 12–14.
(19) Zhang, L.; Qiao, Z.-A.; Zheng, M.; Huo, Q.; Sun, J. *J. Mater. Chem.* **2010**, *20*, 6125–6130.
(20) Du, Y.; Luna, L. E.; Tan, W. S.; Rubner, M. F.; Cohen, R. E. *ACS Nano* **2010**, *4*, 4308–4316.
(21) Stöber, W.; Fink, A.; Bohn, E. *J. Colloid Interface Sci.* **1968**, *26*, 62–69.
(22) Moller, K.; Kobler, J.; Bein, T. *J. Mater. Chem.* **2007**, *17*, 624–631.
(23) Du, X.; He, J. *Langmuir* **2010**, *26*, 10057–10062.
(24) Feng, Z.; Li, Y.; Niu, D.; Li, L.; Zhao, W.; Chen, H.; Li, L.; Gao, J.; Ruan, M.; Shi, J. *Chem. Commun.* **2008**, 2629–2631.
(25) Qiao, Z.-A.; Zhang, L.; Guo, M.; Liu, Y.; Huo, Q. *Chem. Mater.* **2009**, *21*, 3823–3829.
(26) Zhang, X.-T.; Sato, O.; Taguchi, M.; Einaga, Y.; Murakami, T.; Fujishima, A. *Chem. Mater.* **2005**, *17*, 696–700.
(27) Wenzel, R. N. *Ind. Eng. Chem.* **1936**, *28*, 988–994.

(28) Bico, J.; Marzolin, C.; Quere, D. *Europhys. Lett.* **1999**, *47*, 743−747.
(29) Bico, J.; Tordeux, C.; Quere, D. *Europhys. Lett.* **2001**, *52*, 220−226.
(30) Liu, X.; He, J. *J. Colloid Interface Sci.* **2007**, *314*, 341−345.
(31) Du, X.; Li, X.; He, J. *ACS Appl. Mater. Interfaces* **2010**, *2*, 2365−2372.
(32) Li, X.; Du, X.; He, J. *Langmuir* **2010**, *26*, 13528−13534.